Analytica Chimica Acta 1424 (2026) 346203

Contents lists available at ScienceDirect

Analytica Chimica Acta

journal homepage: www.elsevier.com/locate/aca

ESI-Orbitrap MS enables reliable lead isotopic measurements in lake sediment cores

Gianluca Roncoroni [a], Alessio Giussani [a], Andrii Tupys [b,c], Jakub Karasiński [b], Ewa Bulska [b], Nils Johannes Kuhlbusch [d], Andreas Hilkert [d], Damiano Monticelli [a,*]

[a] Department of Science and High Technology, Università of Insubria, Via Valleggio 11, Como, 22100, Italy
[b] Faculty of Chemistry, Biological and Chemical Research Centre, University of Warsaw, Żwirki i Wigury 101, Warsaw, 02-093, Poland
[c] Faculty of Environmental Sciences and Natural Resource Management, Norwegian University of Life Sciences (NMBU), Høgskoleveien 12, Ås, 1433, Norway
[d] Thermo Fisher Scientific, Hanna-Kunath-Straße 11, Bremen, 28199, Germany

HIGHLIGHTS

- First ESI-Orbitrap metal ion isotope ratios (IRs) in complex environmental samples.
- Lake Como sediments were analyzed after digestion and purification.
- Lead IRs measured by ESI-Orbitrap and validated *vs* MC-ICP-MS.
- Leaded gasoline identified as the main legacy Pb contamination source.
- Paves the way towards ESI Orbitrap determination of IRs in real-world samples.

GRAPHICAL ABSTRACT

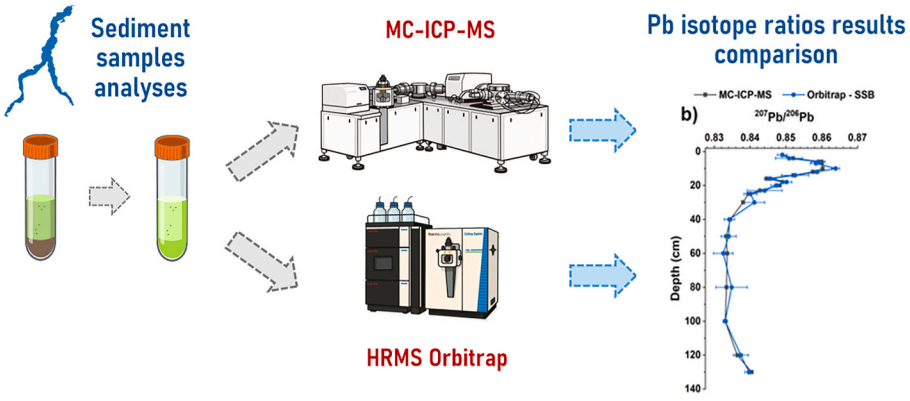

ARTICLE INFO

Keywords:
ESI-Orbitrap IRMS
Pb isotope ratios
Metal–ligand complexation
Validation
Environmental matrix
MC-ICP-MS

ABSTRACT

Background: High resolution mass spectrometry, and particularly Orbitrap based instrumentations, are emerging as powerful technologies for speciation analysis, mainly to collect reliable information on isotope ratios (IRs). During recent years, traditional, stable isotopic systems, namely H, C, N, O and S have been investigated, but we only recently demonstrated that a dedicated complexation procedure followed by collisional dissociation may enable the investigation of metal ion IRs, and particularly lead, employing a standard electrospray ionization source. The procedure has not yet been demonstrated to be applicable to real-world samples.

Results: A total of 31 sediment samples from Lake Como were analyzed for lead IRs by both ESI-Orbitrap and Multi collector ICP-MS. Minor modifications to the original ESI-Orbitrap method, including increased ligand concentration, were required due to sample complexity; the simple Standard–Sample Bracketing (SSB) procedure was demonstrated to be effective in correcting the mass bias. Bland–Altman analysis showed no statistically significant differences between the two methods (95% confidence level) for the two isotope ratios $^{204}Pb/^{206}Pb$ and $^{207}Pb/^{206}Pb$, while a small deviation (<2‰) was observed for the $^{208}Pb/^{206}Pb$, remaining acceptable for

* Corresponding author.
E-mail address: damiano.monticelli@uninsubria.it (D. Monticelli).

https://doi.org/10.1016/j.aca.2026.346203
Received 10 June 2026; Received in revised form 26 August 2026; Accepted 30 August 2026
Available online 31 August 2026

environmental applications. The isotopic data trend identified leaded gasoline as the main contributor to lead contamination in Lake Como during the period 1950-2000.

Significance: This work presents the first reported application of ESI-Orbitrap-based metal isotopic analysis in complex environmental matrices. Factors influencing accuracy and precision were systematically evaluated, demonstrating robust analytical performance. The results establish the potential of the ESI-Orbitrap approach for determining isotope ratios of metal ions in real-world samples.

1. Introduction

The ion trap mass spectrometer commercialized under the name Orbitrap [1] has attracted interest in the field of isotope ratio measurements in recent years [2]. Though being traditionally used in bioanalytical applications, it shows several advantageous features, including versatility, automation capability, simultaneous acquisition over a requested mass range, and especially high resolving power, at least 120,000 at m/z equal to 200 [3], thus promising, when required, the instrumental resolution of isobaric interferences and potentially mitigating the need for chemical approaches. Up to now, applications reported in the literature include small inorganic ions (e.g. nitrates [4], phosphates [5], sulphates [6], perchlorates [7]), as well as organic molecules [8,9], enabling both compound-specific and position-specific determination of isotope ratios (IRs) [3].

Nevertheless, the study of isotopic systems other than H, C, N, O, and S using Orbitrap seems to be underrepresented: lower concentrations and the subtle variability typical of natural environments undoubtedly hinder the application of these procedures to the determination of metal ion IRs.

A more decisive limitation, however, lies in the mass spectrometer itself: high-resolution mass spectrometers are primarily designed for the analysis of organic molecules; consequently, the ion sources compatible with Orbitrap mass analyzers limit their direct applicability to metal ions.

Marcus et al. overcame this issue by coupling the Orbitrap with the Liquid Sampling – Atmospheric Pressure Glow Discharge [10], a custom-made source for microplasma-based ionization. Initially, they reported on the determination of uranium IRs [11], but they also demonstrated that this approach could be applied to several other isotopic systems (e.g. Rb/Sr [12], Nd/Sm [13], Pu [14]). Nevertheless, to the best of our knowledge, the possibility of applying the procedure to complex environmental or biological matrices was not investigated. Moreover, this strategy needs a non-commercially available ionization source, different from the one typically coupled to Orbitrap instruments, namely electrospray (ESI).

As an alternative, we recently introduced the idea that the isotope ratios of several metal cations can be determined by employing a standard ESI source, provided the ions are complexed by an organic ligand. The isotopic pattern of the elements is then obtained by freeing the ion through collisional dissociation before actual detection in Orbitrap [15]. We have demonstrated proof of principle for the determination of lead isotope ratios, but real-world samples are still missing to be investigated.

Here we demonstrate for the first time that the ESI-Orbitrap MS procedure provides reliable data for lead IRs in a complex matrix, namely 31 samples from two sediment cores from Lake Como. Acquisition parameters and mass bias correction strategy ensuring optimal results in terms of accuracy and precision were recognized. Accuracy was assessed by comparing the results obtained on the same samples by Multi Collector Inductively Coupled Plasma Mass Spectrometry (MC-ICP-MS) as a reference procedure, demonstrating the feasibility of lead IRs determination by ESI-Orbitrap on real-world, complex matrix samples.

2. Materials and methods

2.1. Samples, sample treatment procedures and MC-ICP-MS analysis

Thirty-one lacustrine sediment samples from Lake Como, collected by coring at two different locations, were selected as environmental samples to evaluate the effectiveness of ESI-Orbitrap for the determination of Pb isotope ratios in complex natural matrices. Further details are provided in the *Sampling details and core descriptions* section in the Supplementary Material.

As a first treatment, the sediments underwent microwave-assisted acid digestion (ETHOS UP Microwave Digestion System, Milestone, Sorisole, Italy) in two steps, following conventional procedures (see Supplementary Material, section *MW-assisted acid digestion*). The concentration of Pb and of potential interfering species (namely Hg and Tl) was determined in the resulting solutions by single-quadrupole ICP-MS, using the NexION 300D (PerkinElmer, Waltham, MA) instrument (see Supplementary Material, section *Pb concentration in digested samples*). Monitoring these species is crucial. Hg represents an isobaric interferent on ^{204}Pb in MC-ICP-MS, but not in the proposed ESI-Orbitrap procedure, as this element does not form detectable complexes with EDTA under the present operating conditions. Tl, in contrast, is added to unknown samples as an internal standard for isotope ratio correction in MC-ICP-MS. As a result, Tl and Hg concentrations were sufficiently low to make pre-treatment procedures for their removal unnecessary.

In contrast, analyte concentrations were not sufficiently high to allow isotope ratio determination in the presence of matrix by MC-ICP-MS (Plasma 3, Nu Instruments, Wrexham, UK). Therefore, to remove the matrix a chromatographic purification of Pb was performed using a strong anion-exchange resin, according to Tappe et al. [16], with minor modifications. Subsequently, Pb recovery was measured highlighting quantitative separation, as recommended to avoid Pb chromatographic fractionation (see *Pb chromatographic purification procedure and recovery assessment*, Supplementary Material).

The purified samples were evaporated and re-dissolved in a 1% nitric acid. After appropriate dilution and addition of Tl as an internal standard (NIST SRM 997), Pb isotope ratios were measured by MC-ICP-MS: see *MC-ICP-MS analysis* in the Supplementary Material and Table S1.

2.2. Sample preparation for ESI-Orbitrap analysis

The solutions obtained after digestion and purification, as reported above for the determination of Pb IRs by MC-ICP-MS, were further processed to make them compatible with Orbitrap analysis and the proposed analytical strategy. In fact, the MC-ICP-MS analytical solution contains 1% nitric acid, making it unsuitable for injection into the Orbitrap system. Significant amounts of inorganic acids would severely damage both the LC system and the Orbitrap mass spectrometer. Consequently, it is necessary to use mixtures that are compatible with this bioanalytical platform. To this end, an appropriate aliquot of each solution ensuring a final Pb concentration of 500 μg/kg was completely evaporated in PFA vessels, ensuring both solvent exchange and analyte preconcentration. Preconcentration factors ranged from 1.1 to 3.8, with an average value of 2.6. The resulting solid residue was then re-dissolved in the same vessel by adding 20 μL of 50 mM HNO_3 (ultrapure acid was produced using Milestone DuoPUR Subboiling distillation system following the procedure described in Ref. [17], starting from HNO_3 65%

Carlo Erba, for analysis-ISO). Final solutions for ESI-Orbitrap analysis were prepared by adding 1 mL of a 1:1 mixture of MeOH (Carlo Erba, LC/MS grade) and H_2O (ultrapure, produced using a Merck MilliQ EQ 7008 system) containing 5 mM ammonium acetate buffer, prepared from an ammonium hydroxide solution (TraceSELECT Ultra, for trace analysis, $NH_3 \geq 25\%$ in H_2O, Fluka) and acetic acid (puriss. p.a., Fluka). Finally, a 37.5 mM EDTA solution (Merck, extra pure, ≥98%) was added as a complexing agent at a final concentration of 1.5 mM; a Tl(III) solution, prepared from the corresponding nitrate trihydrate salt (Sigma-Aldrich), was added when necessary (see below). The solution was sonicated and finally transferred into 1.5 mL glass vials for analysis. Isotopic standard solutions were prepared following the same procedure, by evaporating appropriate aliquots of a solution containing the NIST SRM 981 Pb isotopic standard (National Institute of Standards and Technology, Maryland, USA).

2.3. ESI-Orbitrap analysis

All measurements were carried out using an Orbitrap Exploris 120™ (Thermo Fisher Scientific) fitted with an OptaMax NG™ ion source and a Heated-ESI probe (Thermo Fisher Scientific). The system includes a quadrupole for MS^1 ion selection and an ion routing multipole used for higher energy collisional dissociation (HCD) with nitrogen gas, followed by the Orbitrap mass analyzer. The mass spectrometer was interfaced with a Vanquish Core HPLC system including a Vanquish Autosampler VC-A12-A (Thermo Fisher Scientific) equipped with a 1000 μL sample loop. The LC system was employed solely for sample introduction, and no chromatographic column was used.

The LC conditions, ion source settings, and mass scan parameters, optimized in our previous work [15], are summarized in Table S2. Briefly, complex selection was performed using a 14 amu and a 20 amu isolation window when measuring Pb alone or Pb and Tl, respectively. The AGC target value was partially modified with respect to our previous work when necessary. The AGC target values tested in this work were 35%, 50%, and 100%. Fragmentation was performed in the HCD cell at its highest energy (200%, equal to 132 V), achieving quantitative conversion of Pb-EDTA into free Pb. In-source fragmentation (CID) was not used because it provided a much lower yield of free Pb than HCD. Finally, the Orbitrap resolving power was reduced to its minimum value of 15000 because of the absence of isobaric interferences in our system, thereby increasing the scan rate and improving counting statistics.

2.4. ESI-Orbitrap data acquisition and processing

Data acquisition was performed in a fully automated manner using the Xcalibur software (Thermo Fisher Scientific). Preliminary analysis of the raw files was carried out using FreeStyle software (Thermo Fisher Scientific). Data extraction from raw files was performed using the IsoX Software (Thermo Fisher Scientific). Isotope ratios were calculated using the R script provided with the IsoX Software (modified by Nils J. Kuhlbusch), as well as Standard-Sample Bracketing (SSB) for drift correction and referencing. The data processing system extracts the peak intensities of the isotopic masses of interest and converts the intensity signals into ions.incremental, a calculated number of ions for the signal. This value is calculated using the following approximation: ions.incremental = (Intensity/Peak.Noise) × 3 × sqrt(240000/FT.Resolution) × sqrt(Microscans). See Kantnerová et al. for further details on the data processing system [2].

Common Analyte Internal Standardization (CAIS) correction was performed using a Microsoft Excel worksheet, using raw IRs calculated with the aforementioned R script. The equations used for correcting Pb isotope ratios in ESI-Orbitrap measurements (SSB and modified CAIS) are reported in the Supplementary Material, section *Mass bias correction procedures*. Details on the deconvolution method used for environmental interpretation of the results are provided in the Supplementary Material, section *Isotope mixing model for Pb IRs deconvolution*.

3. Results and discussion

3.1. Further methodological developments

Moving from standard solutions to real-world samples requires careful evaluation of possible interferences. The latter are still only partially characterized for C, H, N, S, and O isotope ratio determinations, and remain essentially unknown for metal ions when using ESI-Orbitrap MS [15]. As a first approach, we decided to determine isotope ratios after (partial, see below) matrix separation following the procedure adopted for MC-ICP-MS determination. This strategy also ensures application of the identical-treatment principle, enabling a reliable comparison between the results obtained by the two techniques [18]. Future studies may address the issue of adapting the procedure to samples without matrix separation.

3.1.1. Post-purification matrix assessment to establish proper ligand concentration

Initially, sample elemental composition was determined to assess possible interference sources during IRs determination: matrix effects arising from the presence of other elements are well known to cause mass dependent isotope fractionation during analysis when MC-ICP-MS is employed [19].

Table 1 summarizes, through selected statistical descriptors, the data obtained from ICP-MS analysis of the samples following the purification process. The latter proved effective for most transition elements (generally <50 μg/kg), except for Fe and Zn, which are still present in significant amounts even after treatment. Table 1 also reports the expected concentrations of these two elements in the solutions used for the determination of isotope ratios by Orbitrap, after the preconcentration step required to obtain a final Pb concentration of 500 μg/kg. This Pb concentration was found to be the most suitable for maximizing precision and accuracy, following a careful optimization of several factors (both instrumental and related to the composition of the analytical solution), carried out using certified reference materials for the isotopic composition of Pb, as demonstrated in our previous work (see Roncoroni et al. [15]).

Fe and Zn do not represent isobaric interferences in the determination of Pb; however, they affect the complexation of Pb by EDTA. In fact, though zinc complex with EDTA has a complexation constant of $10^{16.50}$, lower than the lead one ($K_{PbEDTA} = 10^{18.04}$), the Fe(III)-EDTA complex exhibits a formation constant several orders of magnitude higher than those of the two aforementioned elements ($K_{Fe(III)EDTA} = 10^{25.1}$) [20]. Accordingly, the concentration of EDTA was increased up to 1.5 mM – 7.5 times higher than the original method [15], to ensure that lead is fully complexed notwithstanding the presence of excess competing iron ions.

3.1.2. Ion injection control: AGC target vs maximum time

The analysis of eight random samples from the two cores – namely

Table 1
Concentrations of Fe and Zn in eluates after performing Pb purification procedure. Expected concentrations are calculated using the preconcentration factor applied to each sample to increase the Pb concentration to the target value of 500 μg/kg.

		Core CO-02		Core CO-09	
		Fe (mg/kg)	Zn (mg/kg)	Fe (mg/kg)	Zn (mg/kg)
Conc. in Pb eluate	Max	22.4	0.82	13.9	0.46
	Min	4.09	0.21	3.15	0.14
	Average	11.7	0.35	5.40	0.33
Expected conc. in solution for ESI-Orbitrap analysis	Max	60.0	1.95	41.1	0.96
	Min	8.99	0.51	4.0	0.40
	Average	33.4	1.01	11.8	0.64

CO-2_2, CO-2_16, CO-2_18, CO-2_40, CO-2_60, CO-2_130, CO-9_24, and CO-9_80 – were initially performed setting the Automatic Gain Control (AGC) target at 100% (accumulation of maximum one million charges in the C-Trap) and a maximum injection time of 1000 ms, in accordance with the optimization procedure performed in our previous work [15]. Data acquired using these settings showed systematic deviations from the reference, MC-ICP-MS values (see Fig. 1, Injection time). A careful examination of the scan parameters revealed that the injection of the ion packet was determined in all cases by the maximum ion injection time of 1000 ms. Conversely, reducing the AGC target to 50% (500k charges in the C-Trap) fixed the number of ions by preventing the maxing out of the ion injection time. Data acquired under these updated AGC settings (see Fig. 1, AGC target) were in agreement with MC-ICP-MS ones. These results clearly indicate that ion packets of the same size must be acquired to ensure maximum accuracy: the causes of mass bias, like space-charge effects, become homogeneous across samples and standards, making their correction easier when operating under AGC control. A similar behavior was reported for other isotopic systems [21].

Accordingly, all data were collected by injecting ion packets of the same size for both samples and standards during each measurement session.

3.1.3. Isotopic fractionation correction methods: SSB vs CAIS

Lead isotope ratios in environmental samples with a complex matrix have never been determined using the proposed method, nor more generally by means of ultrahigh resolution mass spectrometry: the most appropriate mass bias correction approach remains to be determined.

Standard Sample Bracketing (SSB), the Common Analyte Internal Standardization (CAIS), and the Russell equation were originally evaluated in the presence of a simulated matrix [15]. The Russell equation was not considered in the present work as it could not efficiently correct the mass bias [15].

Applying these two correction procedures on the same eight samples yielded comparable results, with slightly higher accuracy observed in the case of SSB, see Fig. 2. However, significant limitations were encountered in the application of the CAIS approach: the calibration lines were of insufficient quality and unable to adequately describe the fractionation phenomena occurring in the samples (data not shown). This CAIS model was calibrated using the same isotopic standards employed for SSB, i.e. non matrix matched standards.

A dedicated calibration set for the CAIS method was prepared by including matrix components, namely five standards with variable concentrations of Fe and Zn encompassing the levels found in the samples (see above paragraph 3.1.1): Fe in the range 20–33 mg/kg and Zn in the range 0.25–0.75 mg/kg. The five samples with the highest iron concentration among the 31 used in this work were measured and raw ratios were corrected by the CAIS model calibrated by the five standards. The results in terms of accuracy were not better than the ones obtained by SSB, as already reported in the previous section when using unmatched standards for calibration. Nevertheless, the CAIS model proved unsatisfactory. Firstly, the calibration model showed again limited linearity between the correction factor "*f*" of Pb and Tl, see black squares in Fig. 3. Secondly, f_{Pb} would be extrapolated for the samples, if this

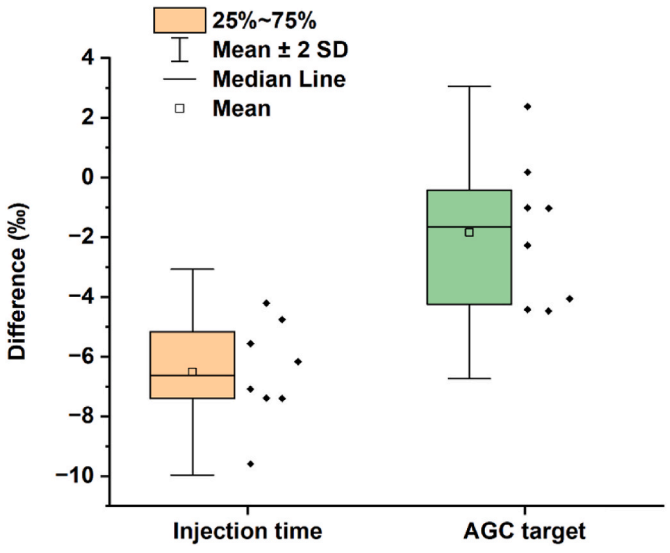

Fig. 1. Comparison of the results obtained for the $^{208}Pb/^{206}Pb$ IR when the injection of ion packets into the Orbitrap is controlled either by reaching the maximum injection time (AGC target equal to 100%, not achieved before the maximum injection time of 1000 ms) or by reaching the AGC target (AGC target equal to 50%, achieved before the maximum injection time of 1000 ms). Data were corrected using the Standard-Sample Bracketing approach. Vertical axis displays the differences between ESI-Orbitrap and MC-ICP-MS isotope ratios expressed as difference in permil (‰) normalized with respect to MC-ICP-MS value: difference ‰ = $(IR_{ESI\text{-}Orbitrap}\text{-}IR_{MC\text{-}ICP\text{-}MS})/IR_{MC\text{-}ICP\text{-}MS}$ * 1000.

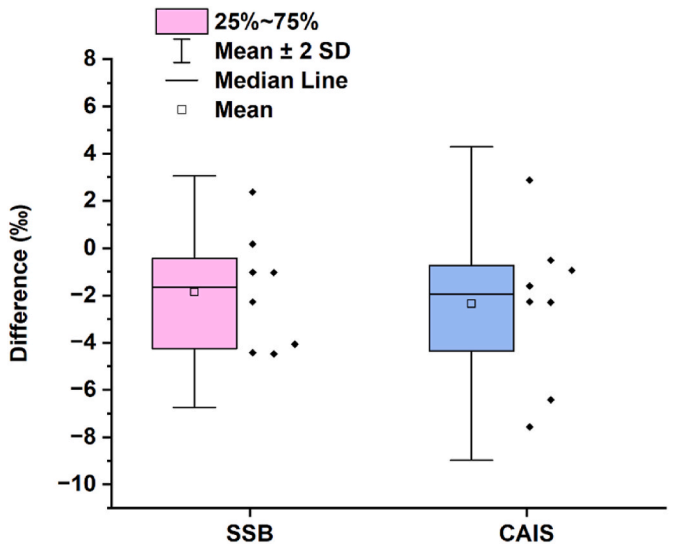

Fig. 2. Comparison of the results obtained for the $^{208}Pb/^{206}Pb$ IR when using SSB or CAIS for mass bias correction. Vertical axis displays the differences between ESI-Orbitrap and MC-ICP-MS isotope ratios expressed as difference in permil (‰) normalized with respect to MC-ICP-MS value: difference ‰ = $(IR_{ESI\text{-}Orbitrap}\text{-}IR_{MC\text{-}ICP\text{-}MS})/IR_{MC\text{-}ICP\text{-}MS}$ * 1000.

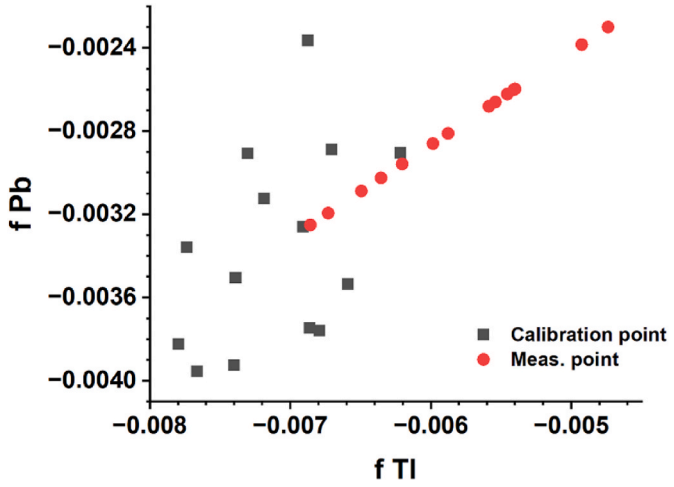

Fig. 3. CAIS calibration system for $^{208}Pb/^{206}Pb$ IR including Fe and Zn standards to simulate the matrix. The linearity of the model is insufficient, and the correction factors f_{Tl} for sediment samples are mainly outside the calibration interval.

model were used, see Fig. 3, red dots. This means that the mass bias for thallium and lead correlate poorly (Pearson's correlation coefficient $r = 0.44$, $p = 0.11$), and thus internal standardization may not be the optimal method for mass bias correction, notwithstanding the attempt to reproduce the matrix components in the calibration solutions (Fig. 3).

Accordingly, the mass bias in environmental samples may not be controlled exclusively by Fe and Zn or these two elements influence Pb and Tl differently, making Tl unsuitable as an internal standard. Moreover, this topic is difficult to investigate because the matrix composition varies among samples, even within the same core. In addition, the chemical composition differs between standards and samples. Free EDTA is the dominant species in the standards, whereas Fe–EDTA complexes dominate in the samples, possibly leading to different matrix effects.

These considerations are particularly relevant because mass bias correction methods used in MC-ICP-MS may not be applicable to ESI-Orbitrap procedures, given the differences in source type and energy (ESI vs ICP), ion beam transmission (accumulation in the C-Trap vs direct), and detection (Orbitrap and Fourier Transform vs Faraday cups or ion counters), which may also result in a different response to matrix effects (or residual matrix effects). This underscores the need for more detailed investigations into matrix-related effects and their impact on the quality of isotopic measurements of real-world samples in ESI-Orbitrap.

Considering these observations, the SSB method was adopted for the processing and correction of the raw isotope ratios in the present work, as it is simpler to apply while providing comparable accuracy to CAIS. The introduction of a fixed and constant ion packet into the mass analyzer seems to efficiently equalize the mass bias between standards and samples.

3.2. Results comparison: ESI-Orbitrap vs MC-ICP-MS

3.2.1. Preliminary considerations

The measured values under optimized conditions are shown in Fig. 4 and compared with the reference values obtained by MC-ICP-MS. All

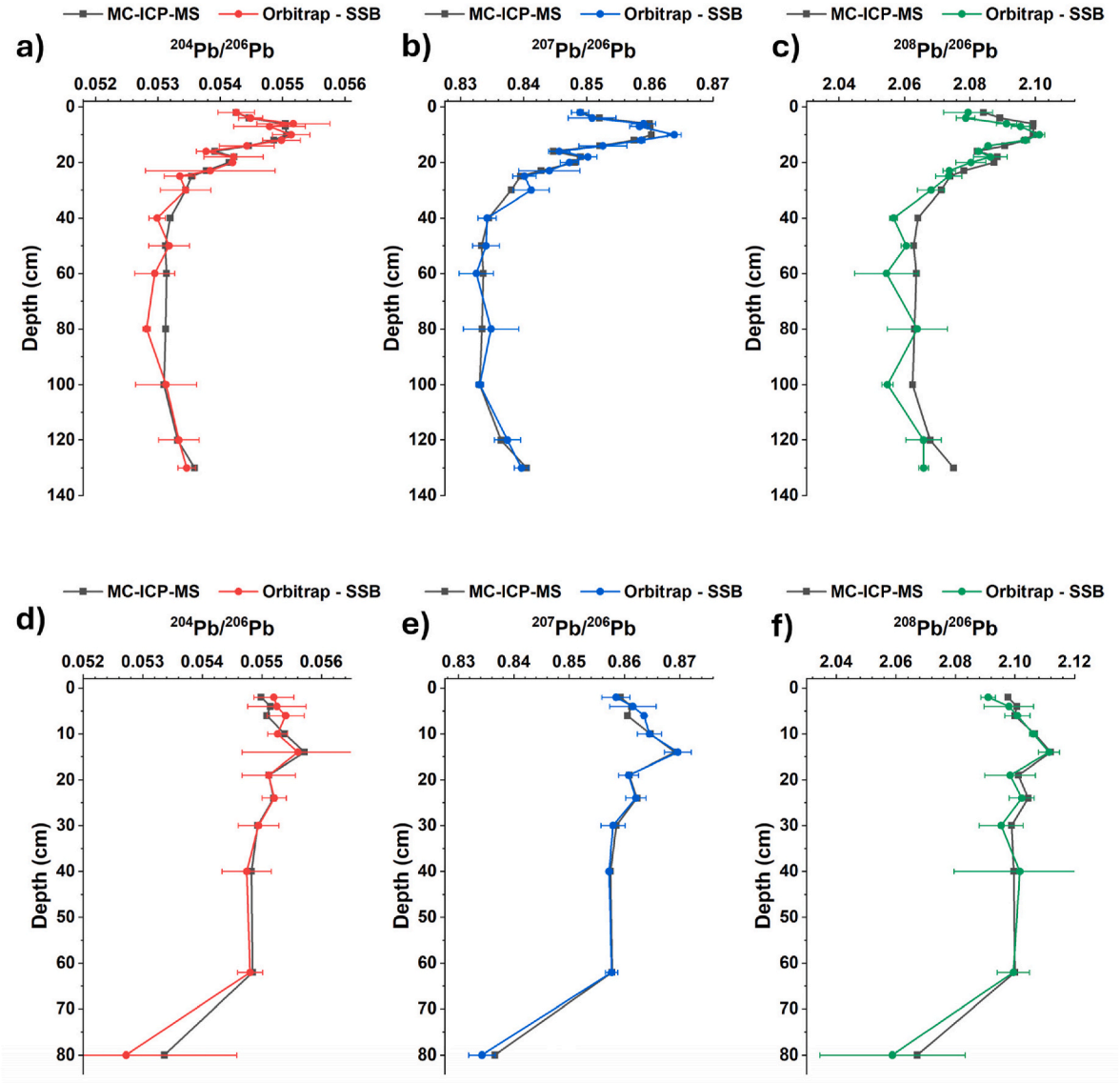

Fig. 4. Comparison between IRs profiles obtained with MC-ICP-MS and ESI-Orbitrap. Panels a), b), and c): core CO-02; panels d), e), and f): core CO-09. Average over three replicates per sample, apart from samples CO-2_14, CO-2_120, CO-9_80, and CO-9_40 (only $^{204}Pb/^{206}Pb$) for which only two replicates were available. Bars represent confidence intervals at 95%. The SDs of the MC-ICP-MS data were determined from 15 replicate acquisitions of the same sample solution during a single analytical session. The average SDs, reflecting instrumental precision only, were 8.10 × 10-7 (0.0015%), 4.14 × 10-6 (0.0005%), and 2.13 × 10-5 (0.0010%) for the $^{204}Pb/^{206}Pb$, $^{207}Pb/^{206}Pb$ and $^{208}Pb/^{206}Pb$ isotope ratios, respectively.

three independent Pb isotope ratios are reported in Fig. 4, expressed with ^{206}Pb as the denominator, for both the CO-02 and CO-09 cores.

Five samples from the CO-02 core – namely 2_23, 2_50, 2_80, 2_100, 2_120 – were acquired under slightly different conditions (results in Fig. 4 for these samples are from these modified conditions). Low sensitivity was initially observed, despite the increased EDTA concentration compared to the original method. This issue was attributed to the particularly high concentration of iron, which exhibits a higher affinity for EDTA than Pb, thus saturating the complexation capacity of the ligand. Further increasing the EDTA concentration, following the same strategy as before, was not considered appropriate, in view of the low volatility of EDTA and the connected risk of its deposition onto the source cone. As an alternative, samples were reanalyzed halving the preconcentration factor, and a solution with a final Pb concentration of 250 μg/kg was analyzed. This adjustment reduced both the concentration of the interferents and the analyte by half; therefore, the AGC target value was lowered to 35% (equivalent to 350k) to keep the measurement under AGC. Only the five samples mentioned at the beginning of the paragraph were reanalyzed under the modified operating conditions.

Precision will be discussed first, followed by trueness.

As per the precision of the measurements, Orbitrap-derived profiles exhibit higher noise, indicating a much lower level of precision compared to MC-ICP-MS data, as we already reported for standard samples [15]. Quantitatively, pooled standard deviations calculated from the full dataset were 0.31%, 0.020%, and 0.0080% for the $^{204}Pb/^{206}Pb$, $^{207}Pb/^{206}Pb$, and $^{208}Pb/^{206}Pb$ ratios, respectively ($n = 31$ for each ratio). This trend is highly consistent with the abundance of Pb isotopes and hence counting statistics: most important, these values are consistent with and show no degradation relative to those previously reported for standard solutions [15], supporting the robustness of the procedure (average values on the three IRs). It is worth noting that the obtained internal precision is close to the shot-noise limit (Fig. 5), suggesting operation near the instrumental limit under the present experimental conditions. As expected, since the achievable precision depends on the number of ions counted, the best and most consistent results were obtained for the $^{208}Pb/^{206}Pb$ and $^{207}Pb/^{206}Pb$ isotope ratios (Fig. 5b and c), which involve the most abundant isotopes (relative errors of 0.44‰ and 0.55‰, respectively). In contrast, the $^{204}Pb/^{206}Pb$ ratio showed a higher relative error of 1.7‰ (Fig. 5a), due to the low relative abundance of isotope ^{204}Pb. More in general, any improvement in precision in the present configuration can only be achieved by increasing the number of measured ions extending the acquisition time, though instrumental drift may limit the actual measurement time.

The precision of the proposed procedure generally compares favorably with quadrupole based (Q-ICP-MS, precision in the 0.1%-0.2% range without separation, see Penanes et al. [22]) and Time of Flight (ToF-ICP-MS) instrumentations (0.2%-0.07% for standard solutions, see Retzmann et al. [23]), but it is one to two orders of magnitude lower than the one of MC-ICP-MS (0.0005%-0.0015% under repeatability conditions for this same dataset, see caption to Fig. 4). Additionally, the latter may use concentrations as low as 1 μg/L (10 μg/L in the present study), whereas the present method, Q-ICP-MS and ToF-ICP-MS operate in the hundreds of μg/L range.

As regards the accordance between ESI-Orbitrap and reference data, the profiles obtained with the two analytical techniques are highly consistent, with excellent agreement in CO-09 and generally very good agreement in CO-02. In the latter, some deviations from the reference values are observed for the $^{208}Pb/^{206}Pb$ ratio (samples at depths of 4, 6, 60, 100, and 130 cm, see below).

The statistical evaluation of the differences for the three IRs in the two cores is reported in Fig. 6 for all the data.

More than 90% of the values (84 out of 93) differ from the reference by ±4‰ or less, with only one clear outlier (sample 9_80, $^{204}Pb/^{206}Pb$ ratio, −12.2‰). Unfortunately, this sample could not be reanalyzed due to sample depletion. Consequently, the underlying cause of this anomaly

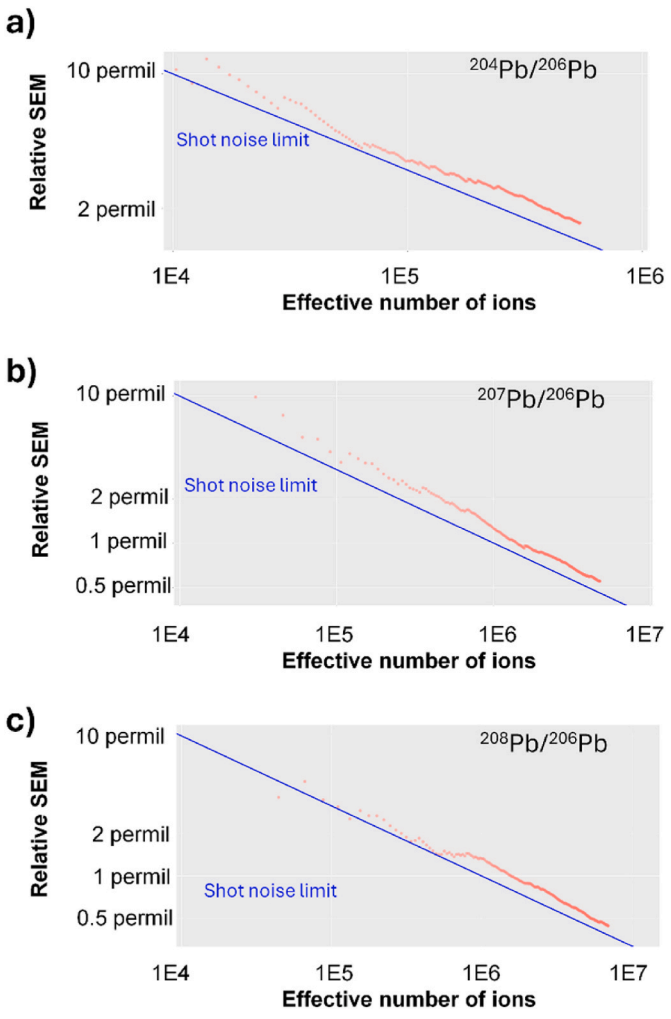

Fig. 5. Shot-noise plot for the isotope ratios a) $^{204}Pb/^{206}Pb$; b) $^{207}Pb/^{206}Pb$; c) $^{208}Pb/^{206}Pb$. Data from a single injection of sample CO-09_24 (AGC = 50%) for a total integration time of 10.5 min.

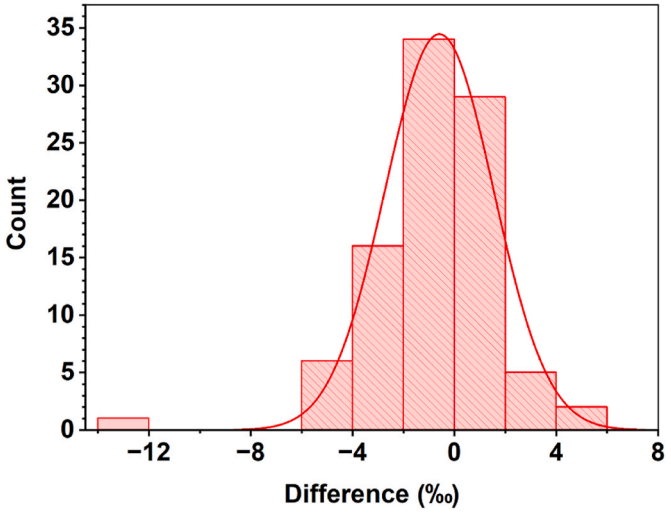

Fig. 6. Distribution of differences between ESI-Orbitrap and MC-ICP-MS isotope ratios expressed as difference in permil (‰) normalized with respect to MC-ICP-MS value: difference ‰ = $(IR_{ESI\text{-}Orbitrap}\text{-}IR_{MC\text{-}ICP\text{-}MS})/IR_{MC\text{-}ICP\text{-}MS}$ * 1000. n = 93 (all isotope ratios measured for 31 sediments). Normal curve is computed using 92 samples, excluding the outlier with difference lower than −12‰.

could not be determined. At present, only speculative explanations can be proposed, including unusually strong matrix effects, instrumental measurement anomalies, or significant environmental contamination.

Excluding this outlier, measurements were normally distributed, according to the Shapiro-Wilk normality test ($n = 92$, $W = 0.98$, $p = 0.17$ and $\alpha = 0.05$), with a mean value of $\mu = -0.60$ and standard deviation $\sigma = 2.13$. Although the mean is close to zero, it indicates a slight tendency toward underestimation relative to MC-ICP-MS values. The deviation from zero was significant at the 95% confidence level, but not at the more stringent 99% confidence level ($n = 92$). Nonetheless, an average difference of −0.6‰ is considered satisfactory and is adequate for most environmental investigations when lead isotopes are involved. Though this small deviation is consistent with the precision of the measurements, a deeper analysis was undertaken to try and better characterize it, especially the deviation in the $^{208}Pb/^{206}Pb$ ratio in core CO-02 (see Fig. 4c).

3.2.2. Bland-Altman analysis

A deeper investigation involving the Bland-Altman approach [24,25] was performed for the three Pb IRs separately: results are reported in Fig. 7.

Fig. 7a shows the results for the $^{204}Pb/^{206}Pb$ isotope ratio. No relevant trend can be observed in the distribution of the differences between the two methods, indicating the absence of effects related to the magnitude of the measured isotope ratio. The zero value is included both within the limits of agreement and within the 95% confidence interval around the mean difference, demonstrating the absence of a statistically significant bias between the two methods. The same considerations apply to the $^{207}Pb/^{206}Pb$ isotope ratio, as shown in Fig. 7b.

Once again, for the $^{208}Pb/^{206}Pb$ isotope ratio (Fig. 7c), no relevant trend in the error is observed. However, the 95% confidence interval around the mean difference does not include zero, indicating the presence of a slight deviation between measured and reference values (on average, equal to −1.7‰, see Fig. 4c and f for a graphical representation of the comparison between the two methods). Nevertheless, zero remains within the limits of agreement (see dashed lines in Fig. 7c): these differences are acceptable for environmental applications involving Pb isotopic measurements, as already mentioned. However, the origin of mass bias phenomena in ESI-Orbitrap remains poorly understood and is generally attributed to space-charge effects and/or signal coalescence. In the absence of clear evidence, it can be hypothesized that these effects, possibly associated with particularly strong matrix effects in some CO-02 samples, underlie the small but statistically significant discrepancy observed relative to the MC-ICP-MS reference values.

Overall, the statistical assessment using Bland–Altman analysis indicates that ESI-Orbitrap provides results statistically consistent with MC-ICP-MS at the 95% confidence level for the $^{204}Pb/^{206}Pb$ and $^{207}Pb/^{206}Pb$ isotope ratios. A small but statistically significant deviation was observed for the $^{208}Pb/^{206}Pb$ ratio; however, its magnitude (<2‰) does not limit the method applicability for studies not requiring the highest level of accuracy as in the present case. Moreover, no indication of proportional error was observed, though the narrow range of IR values may have been insufficient to identify this type of error. The latter observation suggests that the proposed procedure is unlikely to be significantly affected by proportional error, as Pb exhibits one of the largest natural variations in isotope ratios among all elements, making this type of bias easier to detect.

3.3. Paleoenvironmental interpretation

The final phase of this work aimed at identifying the cause of the variation in Pb isotope ratios observed as a function of sediment depth within the cores. At a preliminary level, the variation in Pb isotope ratios occurs consistently with the changes in the total Pb concentration in the sediments (Fig. 8 for the $^{207}Pb/^{206}Pb$ ratio in core CO-02 and Fig. 4 for trends in the other core/IRs). This observation suggests that an external

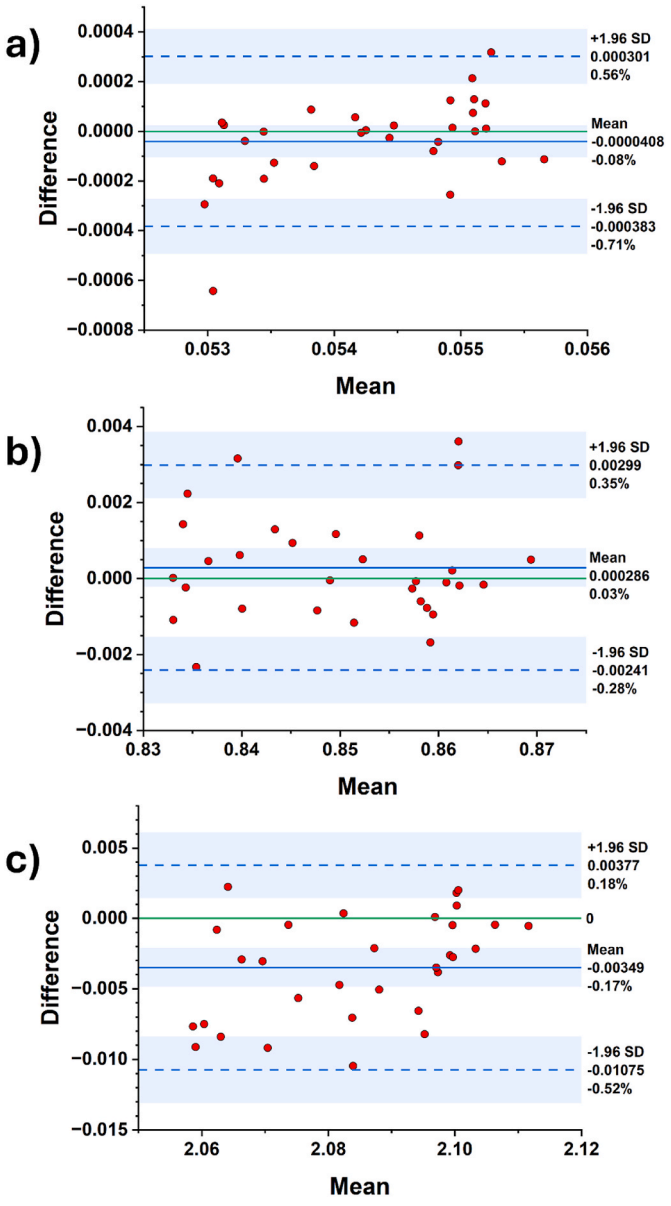

Fig. 7. Bland-Altman plots comparing MC-ICP-MS and ESI-Orbitrap data for a) $^{204}Pb/^{206}Pb$, b) $^{207}Pb/^{206}Pb$ and c) $^{208}Pb/^{206}Pb$. X axis represents the mean value between MC-ICP-MS and ESI-Orbitrap results, while Y axis represents the difference between MC-ICP-MS and ESI-Orbitrap data. Mean value of differences is represented by solid blue lines (MC-ICP-MS value - ESI-Orbitrap value). Intervals of acceptance are delimited by blue-dashed lines. The green line represents zero difference. Shaded blue areas highlight the confidence intervals (95% confidence level) around the mean of differences and limits of agreement. (For interpretation of the references to colour in this figure legend, the reader is referred to the Web version of this article.)

source, characterized by its own isotopic signature, enriched the sediment in Pb.

Two clearly distinguishable intervals can be identified in the trends of the isotope ratios of core CO-02 (see Fig. 8 for the $^{207}Pb/^{206}Pb$ ratio: similar considerations apply to the other two ratios). The isotope ratios remain almost stable and define a background zone in the depth range 30 to 130 cm, whereas a sharp peak is observed in the upper section: the ratios initially increase (between 30 and 10 cm) and subsequently decrease towards the background values. This pattern suggests that the Pb source responsible for the enrichment eventually ceased releasing Pb into the environment.

As opposite, a clear background section cannot be clearly identified

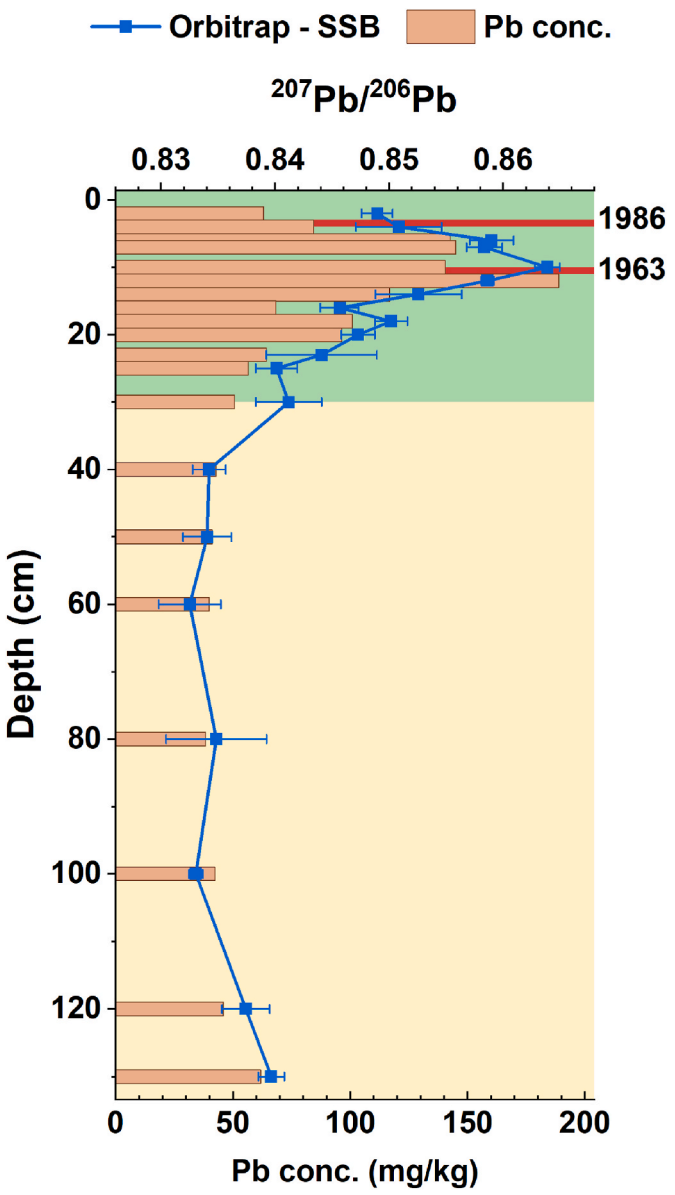

Fig. 8. Pb concentrations in the sediment (brownish bars) and $^{207}Pb/^{206}Pb$ isotope ratio in core CO-02 (blueline). Yellow: background values; green: shift zone where isotope ratios differ from the background values. (For interpretation of the references to colour in this figure legend, the reader is referred to the Web version of this article.)

in core CO-09, see Fig. 4, panels d), e), and f), and a very broad peak is observed, with a maximum at a depth of approximately 14 cm. A decline, though less pronounced, is observed again following the peak values. The absence of a background section is likely related to the location of core CO-09 within the enclosed western branch of Lake Como, characterized by a sedimentation rate of approx. 1.4-1.6 cm/y [26]: the background level was likely not reached within the sampled depth interval of the core and no background correction is possible for this core (see below).

Fig. 9 reports the three-isotope plot with areas identifying common lead sources: the isotope ratio values corresponding to the maxima in both core profiles are reported in the figure together with IRs corresponding to the background zone in core CO-02. As a result, the isotopic signature measured in samples from Lake Como is fully consistent with the isotopic composition of leaded gasoline formerly used in Europe, whereas the background IRs fell between those typically observed for coal and natural lead.

A further refinement was performed for core CO-02 data by applying a simple deconvolution approach, namely subtracting the background contribution (see Supplementary Material, section *Isotope mixing model for Pb IRs deconvolution*). The resulting values, reported in Fig. 9, are consistent with the previous observations and allow for a more robust identification of leaded gasoline as the source of Pb in the lake sediments. No background correction could be performed for core CO-09 due to the absence of a clear background, as described above. The nature of the sediment core itself hinders a more robust identification of the Pb source, as this can only be based on the analysis of the three-isotope plot, thereby partially limiting the environmental interpretation of the data.

Finally, the trend in the isotope ratio and lead total concentration is temporally consistent with the period of maximum use of lead as a fuel additive worldwide (see Fig. S1 and Monticelli et al. [26] for core CO-02 dating by the ^{137}Cs profile). The latter saw an increase up to mid Seventies followed by an initially sharp and then slower decline.

Overall, these findings are consistent with a limited number of literature reports, which have identified lead IRs in lake sediment cores as ideal natural archives for studying lead environmental contamination and its sources [28–30]. The proposed ESI-Orbitrap procedure was demonstrated to provide reliable isotopic data on this natural system.

4. Conclusion

We demonstrated for the first time that the devised ESI-Orbitrap procedure accurately determines Pb isotope ratios in complex environmental matrices, namely 31 samples from two sediment cores collected from Lake Como. Validation was achieved by comparison with the reference technique MC-ICP-MS. Sample preparation for both MC-ICP-MS and ESI-Orbitrap analyses requires an identical number of steps and does not represent a limiting factor for sample throughput. In detail, the $^{204}Pb/^{206}Pb$ and $^{207}Pb/^{206}Pb$ isotope ratios were not statistically different from the reference method, whereas the results for the $^{208}Pb/^{206}Pb$ ratio showed a limited deviation (<2‰). The latter remains within acceptable limits for environmental studies of Pb isotope ratios in complex matrices, though its origin is at present unclear, highlighting the need for an in-depth investigation of matrix-related effects. Despite not being designed for either isotope ratio determination or metal ion analysis, the Orbitrap produced Pb isotope ratios with accuracy comparable to that of MC-ICP-MS, an instrument specifically designed for metal isotope ratio determination. The main limitation of the proposed approach concerns the precision gap between the two techniques: the performance of an optimized, mature, and dedicated methodology is unlikely to be surpassed. Although the present precision is fully adequate for most environmental applications of Pb isotope ratios, at this stage the approach can be effectively extended to applications or isotopic systems that do not require extreme precision (e.g. radiogenic isotopes, isotope tracers, nuclear medicine, and nuclear fuels). Interestingly, precision did not deteriorate when transitioning from standard samples, as observed in our previous work, to real-world samples and remained governed by counting statistics. Accordingly, reducing the aforementioned precision gap with higher-performance techniques will likely depend primarily on improving this parameter.

The analysis of real-world samples highlighted the key factors responsible for accurate results. Firstly, the concentration of the complexing agent should overcome competition by other elements present in the sample matrix, thus enabling the complexation and detection of the analyte. Additionally, introducing the same number of charges in the mass analyzer for both standards and samples proved the key strategy to ensure accuracy: this is a unique feature of the Orbitrap analyzer that limits the space-charge effects. Finally, the Standard-Sample Bracketing (SSB) procedure was demonstrated to be effective in correcting mass bias, achieving results comparable to more complex models like the Common Analyte Internal Standardization (CAIS).

In summary, this work bridges the gap between analytical platforms

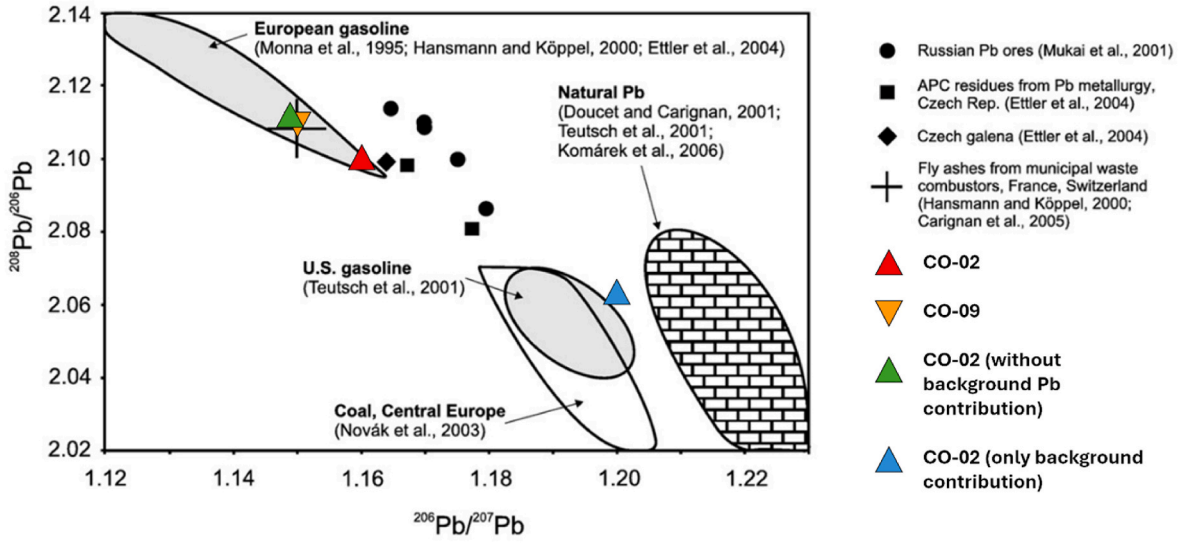

Fig. 9. Three-isotopes plot showing the isotopic compositions of different Pb sources. Reproduced with permission from Komárek et al. [27].

dedicated to bio-related research (e.g. small molecules and omics sciences) and metal isotope ratio determination, paving the way for applying the presented ESI-Orbitrap procedure to real-world samples. This represents an additional application, outside its main field of use, for a widely adopted platform, without requiring hardware modifications to the standard instrumentation. Further investigation is ongoing to better characterize matrix effects and, generally, understanding the sources of mass fractionation to enhance the quality of isotopic data. Extension to other isotopic systems — where high-resolution measurements are critical for resolving isobaric interferences — is also actively being pursued. A particularly interesting application is the possibility to investigate several isotopic systems simultaneously or determine compound specific isotope ratios using the quadrupole to select a single species at a time.

CRediT authorship contribution statement

Gianluca Roncoroni: Writing – original draft, Methodology, Investigation. **Alessio Giussani:** Investigation, Data curation. **Andrii Tupys:** Writing – review & editing, Investigation. **Jakub Karasiński:** Writing – review & editing, Investigation. **Ewa Bulska:** Resources, Funding acquisition. **Nils Johannes Kuhlbusch:** Writing – review & editing, Software, Formal analysis. **Andreas Hilkert:** Writing – review & editing, Investigation. **Damiano Monticelli:** Supervision, Funding acquisition, Conceptualization.

Declaration of competing interests

The authors declare that they have no known competing financial interests or personal relationships that could have appeared to influence the work reported in this paper.

Acknowledgements

Scientific support from the CRIETT center of the University of Insubria (instrument code: MAC15, acquired thanks to funding by Regione Lombardia, Regional Law No. 9/2020, Resolution No. 3776/2020) is greatly acknowledged.

Authors acknowledge the International Lead and Zinc Study Group (ILZSG) for the data on the consumption of lead as a gasoline additive.

Appendix A. Supplementary data

Supplementary data to this article can be found online at https://doi.org/10.1016/j.aca.2026.346203.

Data availability

Data will be made available on request.

References

[1] Q. Hu, R.J. Noll, H. Li, A. Makarov, M. Hardman, R.G. Cooks, The orbitrap: a new mass spectrometer, J. Mass Spectrom. 40 (2005) 430–443, https://doi.org/10.1002/jms.856.

[2] K. Kantnerová, N. Kuhlbusch, D. Juchelka, A. Hilkert, S. Kopf, C. Neubauer, A guide to precise measurements of isotope abundance by ESI-orbitrap MS, Nat. Protoc. (2024), https://doi.org/10.1038/s41596-024-00981-5.

[3] C. Neubauer, K. Kantnerová, A. Lamothe, J. Savarino, A. Hilkert, D. Juchelka, K. U. Hinrichs, M. Elvert, V. Heuer, M. Elsner, R. Bakkour, M. Julien, M. Öztoprak, S. Schouten, S. Hattori, T. Dittmar, Discovering nature's fingerprints: isotope ratio analysis on bioanalytical mass spectrometers, J. Am. Soc. Mass Spectrom. 34 (2023) 525–537, https://doi.org/10.1021/jasms.2c00363.

[4] A. Hilkert, J.K. Böhlke, S.J. Mroczkowski, K.L. Fort, K. Aizikov, X.T. Wang, S. H. Kopf, C. Neubauer, Exploring the potential of electrospray-orbitrap for stable isotope analysis using nitrate as a model, Anal. Chem. 93 (2021) 9139–9148, https://doi.org/10.1021/acs.analchem.1c00944.

[5] N.M. Bernet, C. Soldini, T.M.O. Felder, K. Lapčíková, C. Neubauer, W.L. Queen, R. Kaegi, F. Tamburini, T.B. Hofstetter, Oxygen isotope analyses of phosphate and organophosphorus compounds by electrospray ionization orbitrap mass spectrometry, Anal. Chem. 97 (2025) 22777–22786, https://doi.org/10.1021/acs.analchem.5c04367.

[6] C. Neubauer, A. Crémière, X.T. Wang, N. Thiagarajan, A.L. Sessions, J.F. Adkins, N. F. Dalleska, A.V. Turchyn, J.A. Clegg, A. Moradian, M.J. Sweredoski, S.D. Garbis, J. M. Eiler, Stable isotope analysis of intact oxyanions using electrospray quadrupole-orbitrap mass spectrometry, Anal. Chem. 92 (2020) 3077–3085, https://doi.org/10.1021/acs.analchem.9b04486.

[7] L. Zhu, Y. Hong, S. Hattori, Z. Wang, Z. Wei, Y. Peng, N.J. Kuhlbusch, H. Bao, Sub-10 nanomole perchlorate δ 37 Cl, δ 18 O, and Δ 17 O measurements by ESI-Orbitrap-MS, Anal. Chem. 98 (2026) 6034–6044, https://doi.org/10.1021/acs.analchem.5c06548.

[8] H. Dion-Kirschner, C. Kong-Johnson, K.R. Sharp, N. Dalleska, J.M. Eiler, A. L. Sessions, Position-specific carbon isotope analysis of glucose at natural isotope abundance by electrospray-ionization orbitrap mass spectrometry, Anal. Chem. 98 (2026) 915–926, https://doi.org/10.1021/acs.analchem.5c06166.

[9] H. Kawashima, T. Iezumi, M. Suto, S. Taniyasu, Stable carbon isotope analysis of PFOA and PFOS using orbitrap mass spectrometry, Environ. Sci. Technol. Lett. (2026), https://doi.org/10.1021/acs.estlett.6c00075.

[10] R.K. Marcus, C.D. Quarles, C.J. Barinaga, A.J. Carado, D.W. Koppenaal, Liquid sampling-atmospheric pressure glow discharge ionization source for elemental mass spectrometry, Anal. Chem. 83 (2011) 2425–2429, https://doi.org/10.1021/ac200098h.

[11] E.D. Hoegg, R.K. Marcus, D.W. Koppenaal, J. Irvahn, G.J. Hager, G.L. Hart, Determination of uranium isotope ratios using a liquid sampling atmospheric

pressure glow discharge/orbitrap mass spectrometer system, Rapid Commun. Mass Spectrom. 31 (2017) 1534–1540, https://doi.org/10.1002/rcm.7937.
[12] E.D. Hoegg, S. Godin, J. Szpunar, R. Lobinski, D.W. Koppenaal, R.K. Marcus, Resolving severe elemental isobaric interferences with a combined atomic and molecular ionization source-orbitrap mass spectrometry approach: the 87Sr and 87Rb geochronology pair, Anal. Chem. 93 (2021) 11506–11514, https://doi.org/10.1021/acs.analchem.1c01795.
[13] J.V. Goodwin, S. Shrestha, B.T. Manard, R.K. Marcus, Complete resolution across the neodymium/samarium isotopic envelope with a liquid sampling-atmospheric pressure glow discharge — orbitrap mass spectrometer, Rapid Commun. Mass Spectrom. 38 (2024), https://doi.org/10.1002/rcm.9912.
[14] J.V. Goodwin, B.T. Manard, B.W. Ticknor, P. Cable-Dunlap, R.K. Marcus, Initial characterization and optimization of the liquid sampling-atmospheric pressure glow discharge ionization source coupled to an orbitrap mass spectrometer for the determination of plutonium, Anal. Chem. 95 (2023) 12131–12138, https://doi.org/10.1021/acs.analchem.3c02367.
[15] G. Roncoroni, D. Spanu, G. Binda, D. Monticelli, Metal ion isotope ratio using ESI-orbitrap HRMS: proof of concept and initial performance evaluation for lead isotopic ratios, Anal. Chem. 97 (2025) 13176–13183, https://doi.org/10.1021/acs.analchem.5c01033.
[16] S. Tappe, A. Simonetti, Combined U – pb geochronology and Sr – Nd isotope analysis of the ice river perovskite standard , with implications for kimberlite and alkaline rock petrogenesis, Chem. Geol. 304–305 (2012) 10–17, https://doi.org/10.1016/j.chemgeo.2012.01.030.
[17] D. Monticelli, A. Castelletti, D. Civati, S. Recchia, C. Dossi, How to efficiently produce ultrapure acids, Int. J. Anal. Chem. 2019 (2019) 1–5, https://doi.org/10.1155/2019/5180610.
[18] R.A. Werner, W.A. Brand, Referencing strategies and techniques in stable isotope ratio analysis, Rapid Commun. Mass Spectrom. 15 (2001) 501–519, https://doi.org/10.1002/rcm.258.
[19] L. Yang, Accurate and precise determination of isotopic ratios by MC-ICP-MS: a review, Mass Spectrom. Rev. 28 (2009) 990–1011, https://doi.org/10.1002/mas.20251.
[20] G. Schwarzenbach, Complexometric Titrations, Chapman and Hall, London, 1957.
[21] T.J. Williams, E.D. Hoegg, J.R. Bills, R.K. Marcus, Roles of collisional dissociation modalities on spectral composition and isotope ratio measurement performance of the liquid sampling – atmospheric pressure glow discharge/orbitrap mass spectrometer coupling, Int. J. Mass Spectrom. 464 (2021) 116572, https://doi.org/10.1016/j.ijms.2021.116572.
[22] P.A. Penanes, A.R. Galán, G. Huelga-Suarez, J.Á. Rodríguez-Castrillón, M. Moldovan, J.I. Garcia Alonso, Isotopic measurements using ICP-MS: a tutorial review, J. Anal. At. Spectrom. 37 (2022) 701–726, https://doi.org/10.1039/d2ja00018k.
[23] A. Retzmann, S. Faßbender, M. Rosner, M. von der Au, J. Vogl, Performance of second generation ICP-TOFMS for (multi-)isotope ratio analysis: a case study on B, Sr and Pb and their isotope fractionation behavior during the measurements, J. Anal. At. Spectrom. 38 (2023) 2144–2158, https://doi.org/10.1039/D3JA00084B.
[24] J. Martin Bland, D. Altman, Statistical methods for assessing agreement between two methods of clinical measurement, Lancet 327 (1986) 307–310, https://doi.org/10.1016/S0140-6736(86)90837-8.
[25] D. Giavarina, Understanding Bland Altman analysis, Biochem. Med. 25 (2015) 141–151, https://doi.org/10.11613/BM.2015.015.
[26] D. Monticelli, A. Pozzi, E. Ciceri, B. Giussani, Interpreting complex trace element profiles in sediment cores from a multi-basin deep lake: the western branch of Lake Como, Int. J. Environ. Anal. Chem. 91 (2011) 213–229, https://doi.org/10.1080/03067319.2010.496049.
[27] M. Komárek, V. Ettler, V. Chrastný, M. Mihaljevič, Lead isotopes in environmental sciences: a review, Environ. Int. 34 (2008) 562–577, https://doi.org/10.1016/j.envint.2007.10.005.
[28] H.C. Moor, T. Schaller, M. Sturm, Recent changes in stable lead isotope ratios in sediments of Lake Zug, Switzerland, Environ. Sci. Technol. 30 (1996) 2928–2933, https://doi.org/10.1021/es950895t.
[29] I. Renberg, M.-L. Brännvall, R. Bindler, O. Emteryd, Stable lead isotopes and lake sediments—a useful combination for the study of atmospheric lead pollution history, Sci. Total Environ. 292 (2002) 45–54, https://doi.org/10.1016/S0048-9697(02)00032-3.
[30] L.J. Eades, J.G. Farmer, A.B. MacKenzie, A. Kirika, A.E. Bailey-Watts, Stable lead isotopic characterisation of the historical record of environmental lead contamination in dated freshwater lake sediment cores from northern and central Scotland, Sci. Total Environ. 292 (2002) 55–67, https://doi.org/10.1016/S0048-9697(02)00026-8.